ACS Catalysis

Research Article

pubs.acs.org/acscatalysis

Kinetics and Mechanism of Benzene, Toluene, and Xylene Methylation over H-MFI

Ian Hill,[†] Andre Malek,[‡] and Aditya Bhan*,[†]

[†]Department of Chemical Engineering and Materials Science, University of Minnesota, Minneapolis, Minnesota 55455, United States

[‡]Feedstocks and Energy, The Dow Chemical Company, Freeport, Texas 77541, United States

Supporting Information

ABSTRACT: The methylation of benzene, toluene, *para*-xylene, and *ortho*-xylene over MFI structured H-ZSM-5 and mesoporous self-pillared pentasil (H-SPP) with dimethyl ether (DME) at low conversions (<0.1%) and high DME:aromatic ratios (>30:1) showed linear rate dependencies on aromatic pressure and zero dependence on DME pressure for benzene and toluene. These results are consistent with studies performed for olefin methylation, and are indicative of a zeolite surface covered in DME-derived species reacting with benzene or toluene in the rate-determining step. Saturation in the reaction rate was observed in xylene pressure dependence experiments (at 473 K, <5 kPa xylene); however, enhancement in the reaction rate was not observed when comparing ~1 μm crystallite H-ZSM-5 and 2−7 nm mesopore H-SPP, indicating that xylene methylation proceeds in the absence of diffusion limitations. Simultaneous zero-order rate dependencies on xylene and DME pressures are described by a model based on adsorption of xylene onto a surface methylating species. This model is consistent with observed secondary kinetic isotope effects (k_H/k_D = 1.25−1.35) and extents of d_0, d_3, and d_6 DME formation in the effluent because of isotopic scrambling between unlabeled and d_6 DME when co-fed with aromatics over H-ZSM-5. Post-reaction titration of surface species with water after desorption of physisorbed intermediates showed a 1:1 evolution of methanol to Al present in the catalyst, indicating the presence and involvement of surface methoxides during steady-state methylation of aromatics species.

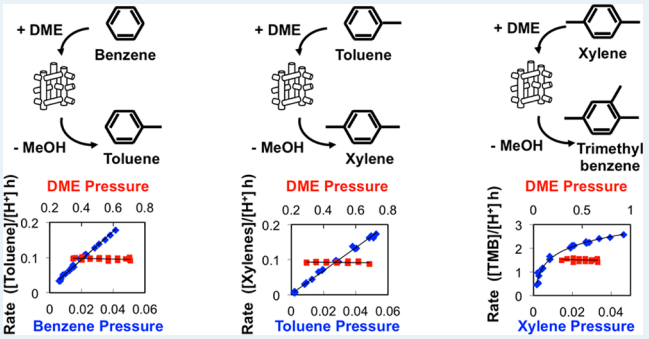

KEYWORDS: *aromatic methylation, H-ZSM-5, mesoporous zeolite, Brønsted acid catalysis, methanol-to-gasoline conversion*

1. INTRODUCTION

Since its discovery in 1977 by Mobil,[1−3] consensus on the mechanism governing the methanol-to-hydrocarbons (MTH) process over zeolite or zeotype catalysts has remained elusive. Despite this, aspects of the MTH chemistry have garnered agreement among researchers. Direct C−C coupling of methanol in MTH is regarded as negligible compared to indirect methylation of olefin and aromatic impurities, as shown via increasing induction periods through rigorous reactant purification,[4] isotopic studies,[5−7] and high activation barriers for direct coupling inferred from computational chemistry studies.[8−10] The development of indirect mechanisms[11−13] has led to the widely accepted "hydrocarbon pool" mechanism,[14−16] which describes the growth, dealkylation, and interconversion of olefin[17−20] and aromatic species[5,21−30] within the confined inorganic framework as being responsible for observed product distributions. Recent work has described the role and contributions of constituent reactions pertinent to MTH chemistry, indicating that the relative rates of these steps yield particular termination products from olefin and aromatic hydrocarbon pools, which can be quantified to determine which cycle is relatively more productive.[31,32]

The use of aromatic co-feeds as a means of studying the evolution of the aromatic hydrocarbon pool has been extensively reported, mainly in using isotopically labeled reagents to track the pathways available for chemical transformations of aromatics, and specifically their role in the formation of light olefins.[25,28,33−35] For example, Mikkelsen et al.[25] have shown through observed isotopic distributions in product olefins in the methylation of aromatics with ^{13}C methanol that all ethene and majority propene are formed through the cracking of arenes on H-ZSM-5, H-MOR, and H-BEA catalysts, and not via the direct coupling of C_1 species. Studies switching from an unlabeled methanol feed to a ^{13}C labeled feed at steady-state MTH conditions have shown that aromatics incorporate ^{13}C at similar rates to ethene and higher olefins incorporate ^{13}C at similar rates to propene indicating that ethene and aromatics, and propene and higher olefins originate from similar reaction steps that are distinct from each other.[33−36] This observation shows that ethene primarily originates from the aromatic hydrocarbon pool, and that the methylation of propene is mostly responsible for the

Received: May 21, 2013
Revised: July 11, 2013
Published: August 5, 2013

formation of higher olefins over SAPO-34,[36] BEA,[33,34] and MFI.[35] The predominant methylbenzenes responsible for the formation of light olefins have been shown to be zeolite framework dependent, and specifically for MFI to comprise C_8−C_{10} aromatics.

The quantitative investigation of the kinetics of aromatic methylation has been a relatively recent focus, and allows for the direct comparison of reaction rates and activation energies between the aromatic and olefin hydrocarbon pools. A comparison of benzene methylation rate parameters with propene methylation[19] run at similar reaction conditions has shown that activation energies (58 and 69 kJ mol^{-1}) and first-order rate constants (4.8 and 4.5×10^{-3} mol g^{-1} h^{-1} $mbar^{-1}$) are similar, and thus the aromatic and olefin hydrocarbon pools are both contributors to the product distribution observed over H-ZSM-5.[37] Recent studies have also quantified the effects of pore size and degree of methylation of co-feed aromatics on the formation rate of light hydrocarbons and higher aromatics.[38] Density functional theory (DFT) calculations using a coadsorbed methanol and toluene precursor over 4T clusters (one alumina and three silica tetrahedra to represent the zeolite) have shown that activation barriers for toluene methylation are of the order of 180−195 kJ mol^{-1}.[39−42] Barriers calculated for the addition of methanol to toluene using hybrid ONIOM methods on 46T clusters of MFI are ∼163 kJ mol^{-1}, showing that framework effects are important in stabilizing MTH intermediates and transition states.[23]

In this work, a quantitative comparison of the kinetics and mechanisms of aromatic methylation to previous work investigating the methylation of C_2−C_4 olefins is provided.[43−45] Rate constants and activation energies have been determined for benzene, toluene, and xylene (BTX) methylation with dimethyl ether (DME) over H-ZSM-5 and mesoporous self-pillared pentasil (H-SPP).[46] Based on the observed kinetics of aromatic methylation we infer the consequences of alkyl substitution on methylation rates in the limit where the coreactant with DME approaches a commensurate size as the zeolite pore. The effects of transport are discussed in light of increasing diffusion limitations with increasing aromatic size. Elementary-step aromatic methylation of benzene, toluene, *para*-xylene, and *ortho*-xylene is investigated to also probe the identity and reactivity of surface species present during aromatic methylation reactions.

2. MATERIALS AND METHODS

Catalyst Preparation. Zeolite H-ZSM-5 (MFI, Zeolyst, Si/Al = 42.6) and self-pillared pentasil (MFI, Si/Al = 75, 2−7 nm mesopores; sample preparation and characterization described elsewhere[46]) were pressed, crushed, and sieved to 180 to 425 μm aggregate sizes. Catalysts were then treated in dry air (1.67 cm^3 s^{-1} NTP, ultrapure, Minneapolis Oxygen) at 773 K for 8 h. Thermal treatment in air was repeated to regenerate self-pillared pentasil (H-SPP) samples between reactions to conserve sample.

Catalysts were diluted in quartz sand (Sigma Aldrich) to 1 g total mass and supported on a quartz frit within a 10 mm quartz U-shaped reactor tube where isothermal reaction conditions were maintained using a National Electric FA120 furnace connected to a 96 Series Watlow temperature controller. Catalyst temperatures were measured using a K-type thermocouple located in a thermowell penetrating the center of the catalyst bed. Samples were treated in flowing He (1.67 cm^3 s^{-1}, ultrapure, Minneapolis Oxygen) at 773 K (0.033 K s^{-1} temperature ramp) for 4 h prior to cooling to reaction temperatures.

Steady-State Aromatic Methylation Reactions. Benzene, toluene, *para*-xylene, and *ortho*-xylene methylation reactions with DME were performed using 1.67 cm^3 s^{-1} total reactant flow rates with 0.68 bar DME (Matheson, CP grade), 0.01 bar aromatic (Sigma Aldrich, 99.9% purity), and 0.03 bar CH_4 (Minneapolis O_2, CP grade) as an internal standard. Methylation reactions over H-ZSM-5 used 50 mg of catalyst at 373 K for benzene, 10 mg catalyst at 403 K for toluene, and 1 mg catalyst at 473 K for xylene to maintain <0.1% aromatic conversion. Methylation over H-SPP used 1 mg catalyst at 473 K for benzene and xylene, and 433 K for toluene co-feeds. Samples of 1 mg of zeolite were achieved using 10 mg of a homogenized 100 mg g^{-1} mixture solid solution with quartz sand, followed by further dilution with quartz sand to 1 g total mass. Pressure dependence reactions were run from 0.002−0.05 bar aromatic and 0.29 to 0.68 bar DME pressures while keeping the partial pressure of the other constant by adjusting He flow rates to maintain 1.67 cm^3 s^{-1} total flow. Products were monitored using an Agilent 5890 gas chromatograph equipped with an HP-1 capillary column attached to an FID detector.

Post-Reaction Zeolite Surface Titration with H_2O. Steady-state methylation reactions were run over 200 mg H-SPP (in the absence of quartz sand diluent) at 358 K for benzene, 343 K for toluene, and 353 K for *para*-xylene co-feeds. After 2 h time-on-stream, flow over the catalyst was switched to 1.67 cm^3 s^{-1} He for 0.5 h to purge residual reactant gases in the reactor lines and catalyst bed and reactor temperature was increased to 423 K at a rate of 0.17 K s^{-1} to remove physisorbed species from the catalyst surface. Flow to the reactor was then switched to 10 kPa H_2O in He with a total flow of 1.67 cm^3 s^{-1} to remove chemisorbed $*CH_3$ species as methanol. Effluent compositions were monitored and quantified using an online Cirrus MKS quadrupole mass spectrometer using CH_4 as an internal standard.

In-Situ d_6 DME/DME Switching. Steady-state methylation reactions over H-SPP were performed at identical catalyst weights, total flow rates, and reaction temperatures as described in the H_2O titration section, with the exception of using 0.20 bar DME pressure instead of 0.68 bar DME. After 2 h time-on-stream, DME composition was changed to 0.10 bar d_0 DME and 0.10 bar d_6 DME for 1 h prior to returning to 0.2 bar d_0 DME. Reaction rates were monitored via GC, and effluent composition was monitored via online MS.

3. RESULTS AND DISCUSSION

The kinetics of benzene, toluene, *para*-xylene, and *ortho*-xylene methylation have been systematically studied to derive reactant pressure and temperature dependencies of the reaction rate at differential reaction conditions in the absence of secondary reactions. Based on these pressure dependencies and rate equations, in conjunction with isotopic[43,44] and surface titration[45] methods used previously, a description of the effect of aromatic substitution on methylation rates has been developed to describe how the mechanistic pathway changes with increasing pressure to one that involves the co-adsorption of the aromatic onto a surface methoxide.

The kinetic relevance of values derived from experiments using 1 mg of catalyst have been considered as reactant stream bypassing catalyst particles can lead to deviations in chemical conversion and, consequently, mechanistic information. Berger et al.[47] have shown that there is no measurable effect of dilution

dx.doi.org/10.1021/cs400377b | ACS Catal. 2013, 3, 1992−2001

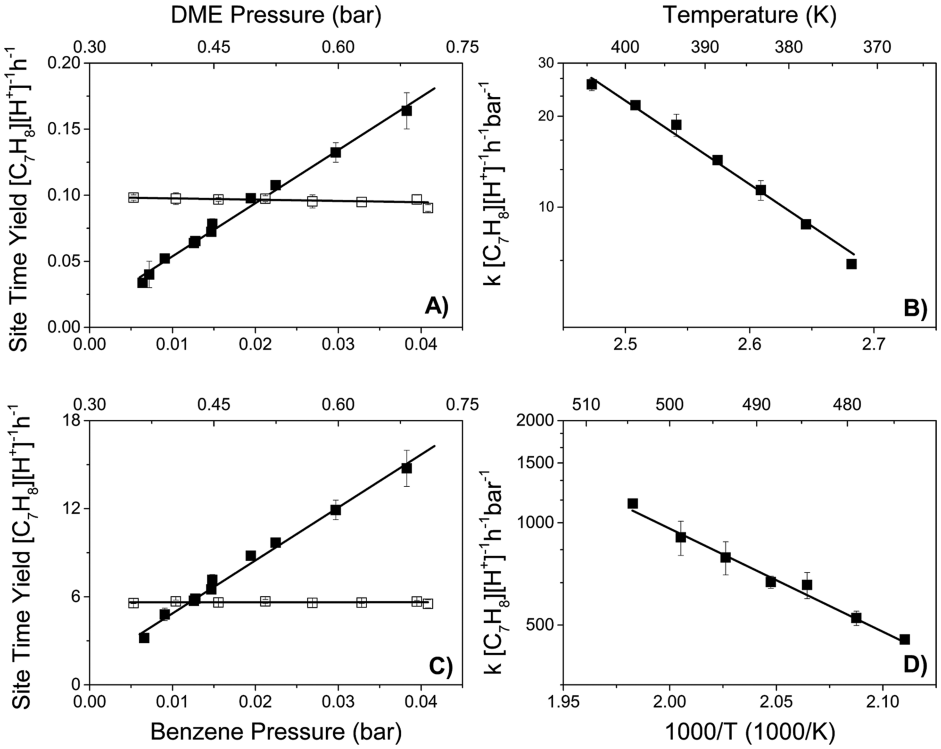

Figure 1. DME methylation of benzene over H-ZSM-5, 50 mg at 373 K, (A and B) and H-SPP, 1 mg at 473 K (C and D). Benzene pressure dependence (■) and DME pressure dependence (□) are shown in the left panels, temperature dependence is shown in the panels to the right.

for an irreversible first order reaction at conversions less than 10% through a systematic investigation of deviation of chemical conversion caused by dilution of the catalyst bed with inert particles in gas−solid systems. As the conversions in this study were kept below 0.1% and previous work has shown that olefin methylation systems proceed via irreversible first-order kinetics over H-ZSM-5[43−45] the scenario detailed by Berger et al.[47] is directly applicable to the kinetics discussed in this work.

Benzene Methylation on H-ZSM-5. The methylation of benzene with DME yielded first-order pressure dependence in benzene and zero-order dependence in DME (Figure 1, panels A and B). These pressure dependencies are consistent with the rapid formation and predominant surface coverage of DME-derived species that react with benzene in the rate-determining step, as observed for C_2-C_4 methylation with DME or methanol.[19,20,43−45] First-order rate constants and activation energies (Table 1) show an identical activation energy and a rate constant within a factor of 0.72 of studies that were performed with 0.037 bar methanol and 0.017 bar benzene at 623 K over H-ZSM-5, where parameters were derived by extrapolating conversions to zero contact time with the catalyst.[37]

Table 1. Apparent Activation Energies and Rate Constants at 373 K for Aromatic Methylation Reactions over H-ZSM-5 and H-SPP[a]

		H-ZSM-5		H-SPP	
		E_a (kJ/mol)	k_{373} (h bar)$^{-1}$	E_a (kJ/mol)	k_{373} (h bar)$^{-1}$
benzene		58 ± 3	6.8	58 ± 2	8.3
toluene		52 ± 4	48.1	47 ± 3	31.4
para-xylene	0.05 bar			44 ± 4	12.5
	0.003 bar	62 ± 3	13.4	62 ± 3	10.1
ortho-xylene	0.05 bar			34 ± 3	3.0
	0.003 bar	62 ± 4	3.1	63 ± 4	4.0

[a]Listed pressures denote xylene reactant pressure at which temperature dependence reactions were run.

A comparison with DFT calculations performed using hybrid functionals[48,49] and previous experimental studies[19,43] shows that benzene methylation proceeds with similar apparent activation barriers (62−77 kJ mol^{-1}) and rate constants (3.7−5.8 $[C_4H_8][H^+]\,h^{-1}\,bar^{-1}$ at 373 K) as propene methylation. The similar rate of propene and benzene methylation could be explained through similarities in the local structure of the two molecules, namely, the secondary substitution about the carbocation formed upon methylation in the absence of additional alkyl substituents to inductively donate electron density. This result is not intuitive on the basis that apparent barriers include adsorption enthalpies, which are calculated to be −94 kJ mol^{-1} at the wB97x-D/6-31 +g(d) level of theory[37] for benzene and −53 kJ mol^{-1} using MP2/DFT with periodic boundary conditions[49] for propene on H-ZSM-5, indicating a greater intrinsic barrier for benzene methylation by ∼40 kJ mol^{-1} compared to that of propene. Experimental enthalpies of adsorption obtained by generating adsorption isochores in low dead-volume systems estimate that benzene has a heat of adsorption of −55 to −75 kJ mol^{-1} on H-ZSM-5, depending on unit cell loading;[50,51] however these values represent an upper bound compared to propene adsorption, and this study reflects adsorption on a Brønsted acid site rather than co-adsorbing on surface-bound methanol-derived species. The noted consistency in benzene and propene methylation rates on HMFI results in part because of the higher adsorption and hence, higher surface coverage of benzene at comparable temperature and pressure conditions.

Toluene Methylation on H-ZSM-5. Toluene methylation with DME over H-ZSM-5 showed first-order dependence in

dx.doi.org/10.1021/cs400377b | ACS Catal. 2013, 3, 1992−2001

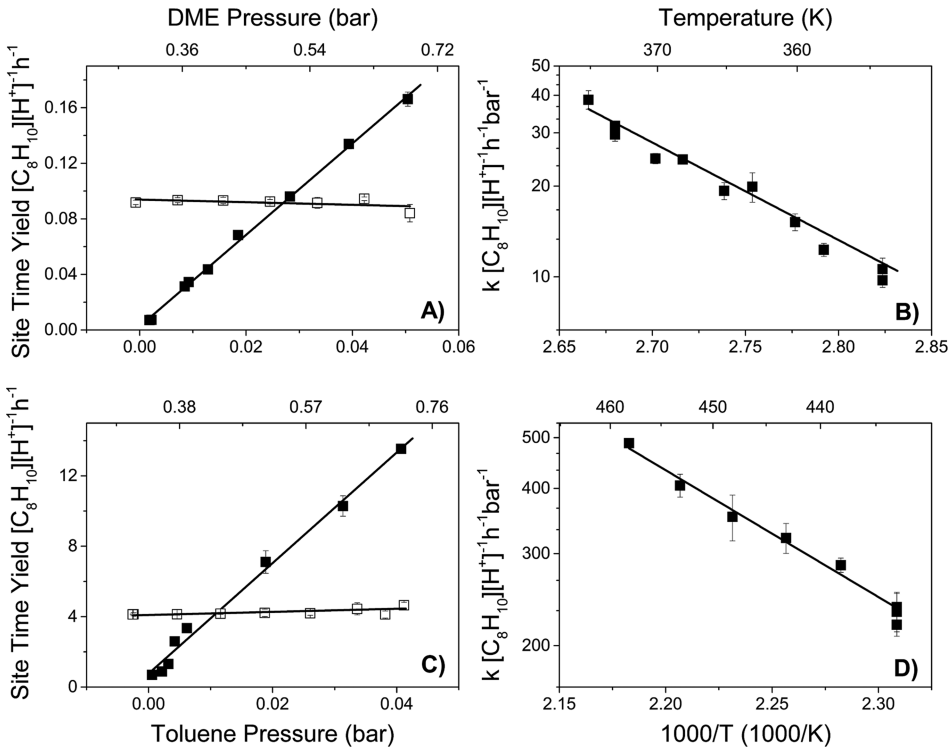

Figure 2. DME methylation of toluene over H-ZSM-5, 10 mg at 403 K, (A and B) and H-SPP, 1 mg at 433 K (C and D). Toluene pressure dependence (■) and DME pressure dependence (□) are shown in the left panels, temperature dependence is shown on the panels to the right.

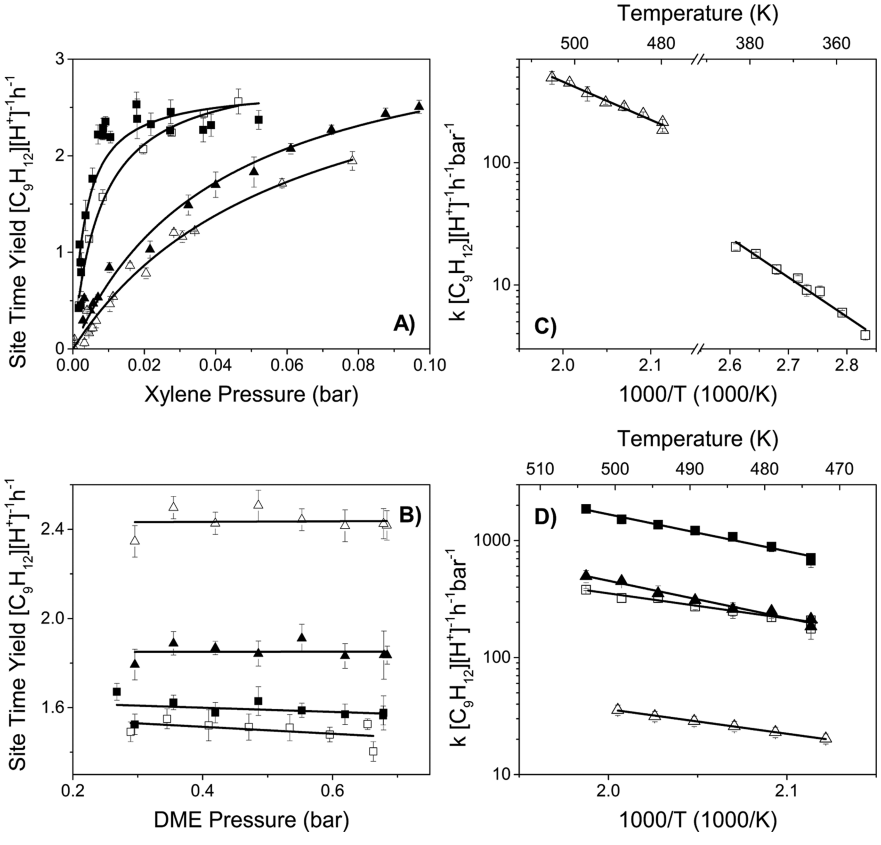

Figure 3. (A) Xylene pressure dependencies for *para*-xylene over H-MFI(□) and H-SPP(■), and *ortho*-xylene over H-MFI(Δ) and H-SPP(▲). (B) DME pressure dependencies for *para*-xylene over H-MFI(□) and H-SPP(■), and *ortho*-xylene over H-MFI(Δ) and H-SPP(▲). (C) Temperature dependence of DME methylation of *para*-xylene over 1 mg H-ZSM-5 (□) and *ortho*-xylene over 1 mg H-ZSM-5 (Δ). (D) Temperature dependence of DME methylation over 1 mg H-SPP at 0.002 bar *para*-xylene (■), and 1 mg H-SPP at 0.05 bar *para*-xylene (□), and 1 mg SPP at 0.002 bar *ortho*-xylene (▲), and 1 mg SPP at 0.05 bar *ortho*-xylene (Δ).

dx.doi.org/10.1021/cs400377b | *ACS Catal.* 2013, 3, 1992−2001

aromatic and zero-order dependence in DME partial pressures in agreement with observed kinetics for benzene methylation, indicating that the zeolite surface is predominantly covered with DME-derived species reacting with toluene in the rate-determining step. The first-order rate constant for toluene methylation on H-ZSM-5 (Table 1) is a factor of 1.5 larger compared to a first-order rate constant calculated from previously reported rates at 373 K, where Vinek et al.[52] co-fed 2.5 kPa toluene and 3.5 kPa methanol over H-ZSM-5 at 373−773 K. Vinek et al.[52] also reported activation energies of 52−85 kJ mol^{-1}, which is in good agreement with 68 kJ mol^{-1} derived from toluene methylation in a simulated riser reactor,[53] 47 kJ mol^{-1} from a fixed fluidized bed reactor from 573−673 K,[54] and 52 kJ mol^{-1} reported in this work (Table 1).

The methylation of toluene proceeds with a rate constant of 48 $[Xylene][H^+]^{-1} h^{-1} bar^{-1}$ at 373 K and agrees well with *n*-butene methylation rate constants of 41−90 $[C_5+C_6][H^+]^{-1} h^{-1} bar^{-1}$,[45] and the activation barrier of 52 kJ mol^{-1} agrees with butene methylation barriers of 44−49[45] and 48[19] kJ mol^{-1} from previous experimental studies. The effective change in kinetics from benzene to toluene are similar to that of propene and *n*-butene, respectively, indicating that the addition of a methyl group in these cases has a similar effect on stabilizing reaction intermediates, namely, inductive electron donation, despite the different extended structure of aromatics compared to olefins.

Toluene heats of adsorption derived from equilibrium isochores over H-ZSM-5[51] range between −60 to −80 kJ mol^{-1}, which is similar to *trans*-2-butene adsorption values of −68 kJ mol^{-1} calculated using MP2/DFT with periodic boundary conditions.[49] This agreement makes a direct comparison of apparent barriers between toluene and butene more relevant than for benzene and propene.

Comparison of Benzene and Toluene Methylation Rates on H-MFI and Mesoporous H-SPP. Aromatic and DME pressure dependencies and temperature dependencies for benzene and toluene methylation over H-SPP are shown in the bottom panels of Figures 1 and 2 for benzene and toluene, respectively. Rate constants agree within 50% and measured activation energies within 10% (Table 1) between microporous and mesoporous MFI samples. This indicates kinetic control for these systems, and any effects of sterics or confinement are strictly limited to the micropores for benzene and toluene methylation.

***Ortho*- and *Para*-Xylene Methylation.** The results of xylene methylation are presented in Figure 3, with kinetic parameters reported in Table 1. While methylation rate constants increased from benzene to toluene methylation reactions over H-ZSM-5, the marked decrease in xylene methylation rate constants is not intuitive, as increasing methyl substitution about the aromatic ring is expected to further increase intermediate carbocation stability. Ahn et al.[38] have recently reported that the rate of methylation from toluene, to *para*-xylene, to 1,2,4-trimethylbenzene decreases from 35, to 22, to 3.7 $[10^{-2}$ mol (mol H s)$^{-1}]$ when feeding 1.2 kPa toluene and 0.3 kPa methanol, a 4:1 aromatic to methanol ratio, at 673 K over H-ZSM-5 at 45−58% conversion. The decrease in methylation rate was ascribed to diffusion limitations in xylenes and larger aromatics in the medium pore zeolites, where these species would mostly dealkylate to lower methylbenzenes with more favorable diffusion properties as opposed to directly leaving the zeolite framework. While reaction rates for *para*- and *ortho*-xylene are independent of DME pressure, as in the case of benzene and toluene methylation, xylene methylation rates saturate with respect to xylene partial pressure at the reaction conditions used in this study (Figures 1−3). The origin of this behavior could arise from (i) diffusion limitations, (ii) a change in the rate-determining step, or (iii) a change in the predominant surface species prior to the rate-determining step.

Diffusion of Aromatics in H-ZSM-5. The diffusion of aromatic molecules in zeolites has been extensively studied using spectroscopy,[55,56] experimental methods,[50,51,57−64] and theoretical calculations.[65,66] The effect of coking on diffusion in zeolites has shown that coking has little effect on the selectivity toward *para*-xylene during toluene methylation reactions on H-ZSM-5 as inferred using infrared (IR) spectroscopy and reaction rate measurements.[55] A model for a zero-length column (ZLC) experimental system, developed by Ruthven and Vidoni,[59] has allowed for this experimental technique to account for combined kinetic effects of surface resistance and internal diffusion limitations to mass transfer. Diffusion coefficients for benzene, *ortho*- and *para*-xylene over H-ZSM-5 and silicalite using ZLC have been calculated using this model for MFI frameworks.[57,58] Calculating Thiele moduli using these values, and toluene diffusivities obtained via TGA,[64] at relevant reaction temperatures and rate constants reported in Table 1, yield the most diffusion-limited case of *ortho*-xylene methylation $\varphi = 0.19$ using 1 μm crystallite sizes, which indicates that the rate constants reported in this work are dictated by reaction kinetics. Thiele moduli calculations are confirmed by the experimental observation that mesoporous and microporous H-SPP and H-ZSM-5 samples saturate at nearly identical rates (2.7 compared to 2.9 h^{-1}) for *para*-xylene methylation. With a >150 fold decrease in the critical diffusion length, the saturation rate achieved with respect to xylene partial pressure indicates that this reaction is operating in kinetically limited regimes.

Temperature Dependence for *Ortho*-Xylene and *Para*-Xylene in Linear and Saturated Rate Regimes. Temperature dependence studies were carried out on H-SPP at 0.003 and 0.05 bar *para*- and *ortho*-xylene pressures. These pressures correspond to linear and saturated regimes in the xylene pressure dependent data, which we ascribe to a zeolite surface predominately covered in surface methoxides and xylene molecules adsorbed on methoxides, respectively. These inferred surface species and experimental evidence for their presence and reactivity will be discussed in studies presented below. High-pressure regimes yielded apparent activation barriers of 34 to 44 kJ mol^{-1} and low-pressure regimes 63 to 62 kJ mol^{-1} for *ortho*- and *para*-xylene, respectively (Table 1). While first-order rate constants between high and low-pressure regimes are within 25% at 373 K, the differences in activation barriers indicate that this agreement is coincidental, as a different choice in reference temperature would cause these values to diverge. Differing apparent barriers for methylation at saturated pressures compared to linear regimes implies either a change in the rate determining step or a change in the predominant zeolite surface species. Considering the same bond to be broken in both cases, the intrinsic activation barrier would remain constant, requiring the saturated regime to have a more stabilized surface species prior to the rate-determining step compared to surface species present in low-pressure regimes.

Post-Reaction Zeolite Surface Titration with H_2O for Benzene, Toluene, and *Para*-Xylene Methylation. Resolving active surface derivatives of DME or methanol for methylation reactions is a continuing debate in the MTH literature, specifically, the formation of co-adsorption complexes from physisorbed reactants or a stepwise mechanism through the

Scheme 1. Three Steps Involved in the Titration of Surface Species Generated in Aromatic Methylation Experiments on H-SPP, where n = 0,1,2

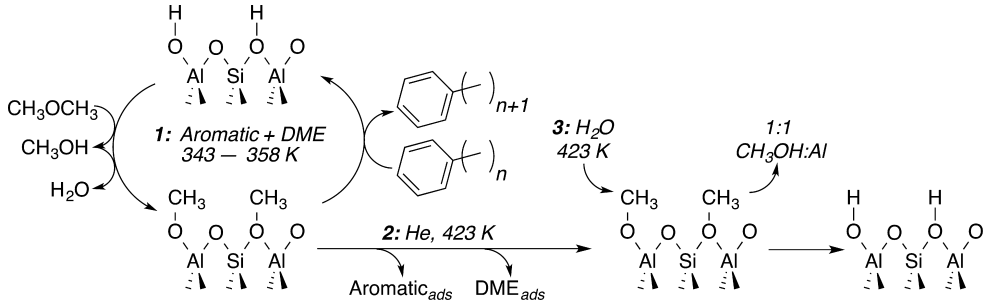

formation of a surface methoxide species.[67] Computational methods have reported consistent results[23,48,49,68] with kinetic measurements[19,20] by modeling methylation reactions via the co-adsorption mechanism. However, FTIR[69] and ^{13}C MAS NMR[70,71] at 453 K and above and computational studies[72,73] evidence the existence of surface methoxides on the zeolite surface. These surface methoxides are unable to desorb, because of the absence of a β-hydrogen, except via reaction, and their stability has been noted up to 673 K under vacuum.[69,70,74] The titration of chemisorbed methoxides on the surface of H-SPP was performed by isolating steady-state MTH surface species in a flow of helium prior to heating to 423 K and introducing water to remove any chemisorbed species.[45] The experimental setup is outlined in Scheme 1, and the results of these chemical titration studies are reported in Table 2. Upon interaction with water,

Table 2. Results for (a) Post-Reaction Water Titration Experiments and (b) Isotopic Switching Experiments over H-SPP[a]

			effluent DME content			
		CH_3*/Al	d_0	d_3	d_6	k_H/k_D
benzene		0.95 ± 0.06	1	1.69	0.86	1.25 ± 0.08
toluene		0.96 ± 0.07	1	1.52	0.82	1.35 ± 0.06
para-xylene	0.05 bar	0.98 ± 0.08	1	0.04	0.84	1.34 ± 0.04
	0.003 bar		1	0.23	0.85	1.31 ± 0.05

[a]Deuterium distributions in effluent DME are normalized to d_0 (m/z = 46) abundances.

0.95−0.98 CH_3OH:Al was evolved after benzene, toluene, and *para*-xylene methylation at two different reactant partial pressures, indicating that, at these conditions, the surface is predominantly covered by surface methoxide species (*CH_3).

In-Situ d_6 DME/DME Switching for Benzene, Toluene, and *Para*-Xylene Methylation. H-SPP samples were exposed to a 50:50 mixture of d_0/d_6 DME after steady-state operation in the absence of deuterated DME. Results for these studies are shown in Table 2 and indicate that the rate-determining step for all BTX methylation reactions involves the formation of a C−C bond in the transition state as inferred from the observed secondary kinetic isotope effect ranging from 1.25−1.35 k_H/k_D. Benzene and toluene methylation reactions showed a near-binomial distribution of d_0:d_3:d_6 DME (1:2:1), consistent with results from ethene methylation from a previous work.[43] In these instances, the binomial distribution of d_0, d_3, and d_6 DME in the effluent indicates a rapid breaking/reforming of C−O bonds of DME upon interaction with the zeolite surface. *Para*-xylene methylation showed ∼15% of the C−O bond scrambling observed in effluent DME compared to benzene and toluene methylation using 0.003 bar partial pressure of *para*-xylene, and almost no scrambling is observed in the presence of 0.05 bar *para*-xylene (Figure 4). This suppressed scrambling could

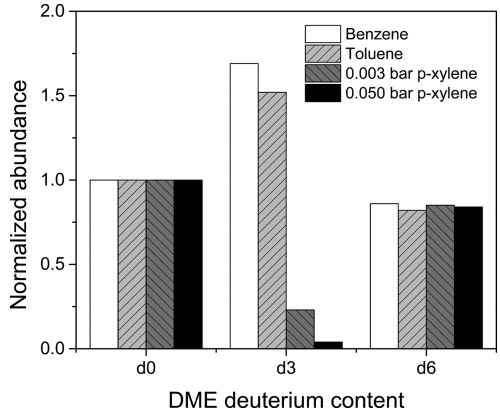

Figure 4. Isotopic scrambling results upon introduction of 1:1 d_6:d_0 DME at steady-state methylation conditions for benzene, toluene, and *para*-xylene methylation.

indicate that surface methoxides are hindered from reacting with other gas-phase DME molecules to facilitate C−O scrambling, which is consistent with *para*-xylene blocking these sites through co-adsorption, which would be expected to exacerbate at higher xylene partial pressures.

Rate Equation for BTX Methylation Systems. The linear pressure dependence of benzene and toluene methylation rates on aromatic pressure and rate independence with respect to DME over MFI indicates a mechanism similar to that previously described for C_2−C_4 olefins over MFI, BEA, MOR, and FER.[43−45] The elementary steps involved for benzene and toluene methylation are described in eq 1, and shown in Scheme 2 (top)

$$\text{(i)}\quad CH_3OCH_3 + H^* \leftrightarrow H{\cdot}CH_3OCH_3^* \quad K_{ads}$$
$$\text{(ii)}\quad H{\cdot}CH_3OCH_3^* \leftrightarrow CH_3OH + CH_3^* \quad K_M$$
$$\text{(iii)}\quad CH_3^* + Ar_n \rightarrow Ar_{n+1} + H^* \quad k \qquad (1)$$

where Ar_n represents an aromatic with n methyl groups, or 0, 1, and 2 for benzene, toluene, and xylene, respectively, and k is the apparent rate constant. The related rate equation, normalized per zeolite framework Al, for this sequence of elementary steps is

dx.doi.org/10.1021/cs400377b | ACS Catal. 2013, 3, 1992−2001

Scheme 2. Proposed Mechanisms for Benzene and Toluene (top) and *Para*-Xylene and *Ortho*-Xylene (bottom) Methylation with DME

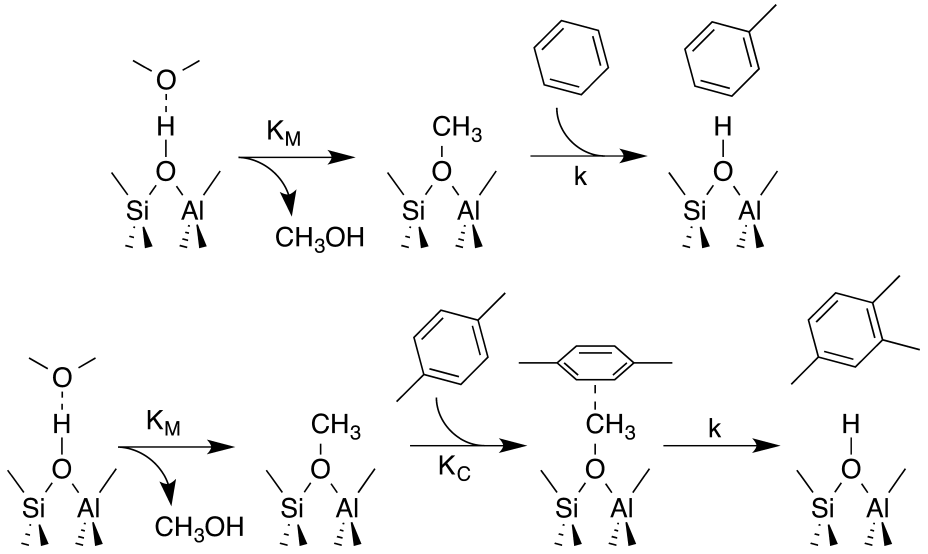

$$\frac{\text{Rate}}{\text{Al}} = \frac{K_{ads}K_M k[\text{Ar}_n]\frac{[\text{DME}]}{[\text{CH}_3\text{OH}]}}{1 + K_{ads}[\text{DME}] + K_{ads}K_M\frac{[\text{DME}]}{[\text{CH}_3\text{OH}]}} \quad (2)$$

Assuming inhibition by methanol is negligible because of its trace quantities observed compared to DME and that methanol is also active for methylation reactions, and the surface is predominately covered by surface methoxides as observed from surface titration studies, eq 2 simplifies to

$$\frac{\text{Rate}}{\text{Al}} = k[\text{Ar}_n] \quad (3)$$

This model fits rate data presented in Figures 1 and 2 for all partial pressures of DME and benzene/toluene measured, as well as observed secondary kinetic isotope effects and surface titration studies.

Based on the observations that (i) the reaction rate simultaneously saturates in xylene and DME pressures for both *para*- and *ortho*-xylene, (ii) the saturated rate for *para*-xylene and *ortho*-xylene methylation does not change appreciably from H-ZSM-5 samples to H-SPP samples, and (iii) observed secondary kinetic isotope effects, we postulate that this system is kinetically limited and the rate-determining step involves a surface species derived from DME and xylene, but still involves the breaking/formation of a C−C bond. Equation 4 outlines a mechanism, which involves the formation of a surface methoxide and the adsorption of a subsequent xylene molecule prior to the rate-determining step (Scheme 2, bottom).

$$\begin{aligned}
&\text{(i)} && \text{CH}_3\text{OCH}_3 + \text{H}^* \leftrightarrow \text{H}\cdot\text{CH}_3\text{OCH}_3^* && K_{ads}\\
&\text{(ii)} && \text{H}\cdot\text{CH}_3\text{OCH}_3^* \leftrightarrow \text{CH}_3\text{OH} + \text{CH}_3^* && K_M\\
&\text{(iii)} && \text{CH}_3^* + \text{Xylene} \leftrightarrow \text{Xylene}\cdot\text{CH}_3^* && K_c\\
&\text{(iv)} && \text{Xylene}\cdot\text{CH}_3^* \rightarrow \text{TMB} + \text{H}^* && k
\end{aligned} \quad (4)$$

The related rate equation for this sequence of elementary steps is

$$\frac{\text{Rate}}{\text{Al}} = K_{ads}K_M K_c k[\text{Xylene}]\frac{[\text{DME}]}{[\text{CH}_3\text{OH}]} \Big/ \left[1 + K_{ads}[\text{DME}] + K_{ads}K_M\frac{[\text{DME}]}{[\text{CH}_3\text{OH}]} + K_{ads}K_M K_c[\text{Xylene}]\frac{[\text{DME}]}{[\text{CH}_3\text{OH}]}\right] \quad (5)$$

Considering the negligible formation of methanol compared to DME as observed in reactor effluents, and the predominant surface species to be surface methoxides or coadsorbed methoxides with xylene, eq 2 simplifies to:

$$\frac{\text{Rate}}{\text{Al}} = \frac{K_c k[\text{Xylene}]}{1 + K_c[\text{Xylene}]} \quad (6)$$

Nonlinear fitting of eq 6 to the pressure dependent data are plotted in Figure 3, and the parameter fits are presented in Table 3. The zero-order rate constant for *para*-xylene saturates at 2.7−2.9 [TMB][H+]$^{-1}$ h^{-1}, and for *ortho*-xylene at 3.5 [TMB][H+]$^{-1}$ h^{-1}. Co-adsorption equilibrium constants are higher for *para*-xylene compared to *ortho*-xylene, and H-SPP samples increase this value compared to H-MFI samples.

Table 3. Parameter Fitting Results for Equation 3 Modeling Xylene Pressure Dependent Data

		K_c	k_{473} ([TMB][H$^+$]$^{-1}$ h^{-1})
para-xylene	H-ZSM-5	130 ± 20	2.9 ± 0.5
	H-SPP	290 ± 70	2.7 ± 0.8
ortho-xylene	H-ZSM-5	17 ± 3	3.5 ± 0.7
	H-SPP	24 ± 4	3.5 ± 0.6

Adsorption Effects of Aromatics in MFI Structures. The distinct aromatic pressure dependence behavior exhibited by xylenes compared to benzene and toluene arises, in part, because of stronger surface adsorption. Brogaard et al.[75] have reported using self-consistent DFT with BEEF-vdW and RPBE functionals and periodic boundary conditions that for MFI structures yield adsorption enthalpies of −59, −73, and −78 kJ mol^{-1} for

dx.doi.org/10.1021/cs400377b | ACS Catal. 2013, 3, 1992−2001

benzene, toluene, and *para*-xylene, respectively. When compared to experimental adsorption enthalpies of −55, −80, and −96 kJ mol^{-1},[76] the computational results progressively underestimated adsorbants with higher degrees of substitution. Brogaard et al.[75] noted that this discrepancy could be possibly due to either underestimates in the van der Waals interactions between methyl groups and the inorganic framework or through effects specific to the choice of Brønsted acid site location used for calculations. Aromatic compounds studied (benzene through tetracene) were found to prefer occupation of channel intersections, however, benzene and toluene were the only adsorbents that had a relative preference to adsorb into the more-restricted sinusoidal channels compared to adsorption in straight channels.[75] This indicates that for xylenes and larger aromatics, accessibility to sinusoidal channels is restricted. These results are supported by IR measurements by Armaroli et al.[56] that show benzene, toluene, *para*-xylene, and *ortho*-xylene completely occupy the acid sites of H-ZSM-5, but *meta*-xylene only partially occupies surface acid sites at room temperature, indicating restricted access to a fraction of these sites, which would be expected to exacerbate with bulkier surface methoxides in place of Brønsted acid sites and could lead to similar behavior in *para*- and *ortho*-xylene.

This restricted accessibility has also been noted experimentally by calorimetric studies obtaining adsorption isotherms for *para*-xylene on H-ZSM-5, noting a phase transition in the zeolite structure at 300 K,[77] thermogravimetric analysis citing 210 and 180 J mol^{-1} K^{-1} entropy differences for *para*-xylene and benzene adsorption, respectively.[78] X-ray diffraction studies for *para*-,[79] *ortho*-, and *meta*-xylene isomers[80] in silicalite have noted missing symmetries indicative of aromatic occupation of sinusoidal channels, in addition to distorting the MFI straight channels to induce a monoclinic to orthorhombic transition at room temperature for aromatic loadings greater than three molecules per unit cell. The preferential occupation of straight channels over sinusoidal channels has been noted to lead to significant kinetic differences in *para*-xylene isomerization compared to *ortho*- and *meta*-xylene isomers over H-ZSM-5, which were mostly invariant with the addition of MgO and CaO on a 1:1 basis with Al, indicating that occupation effects play a larger role than sterics in this system.[81] The less than 2-fold enhanced adsorption on H-SPP compared to H-MFI therefore, could possibly be explained by enhanced access to less favored adsorption sites with less effect of sterics from neighboring molecules, allowing for the achievement of a saturated zeolite surface at lower aromatic partial pressures.

The methylation of xylene on MFI is distinct from elementary-step methylation reactions of olefins, benzene, and toluene in that, in the absence of diffusion limitations, rate saturation is achieved relative to both xylene and DME partial pressures. This phenomenon is attributed to the saturation of the zeolite surface with xylene molecules adsorbing on a surface methoxide, which is not observed for C_2−C_4 olefins and benzene and toluene under nearly identical reaction conditions and chemical conversions.

The product selectivity in methanol-to-hydrocarbons (MTH) conversion can be attributed to the relative propagation of olefin and aromatic methylation and cracking cycles. We report that aromatic methylation pathways for benzene and toluene are identical to those previously reported for olefin methylation and hence, a direct comparison of rate parameters for olefin and aromatic alkylation pathways can be inferred. Chemical titration and isotopic scrambling studies at steady-state methylation conditions evidence the involvement of surface methoxides in both olefin and aromatic methylation cycles. In contrast to the observed increase in olefin methylation rates with increasing substitution about the double bond, aromatic methylation rates do not monotonically increase with increasing methyl substitution implying that the aromatic methylation cycle proceeds under space limitation conditions relative to the olefin methylation cycle.

4. CONCLUSIONS

The rate of methylation of benzene and toluene with DME at temperatures below 503 K at differential conversions is first-order dependent in aromatic pressure and independent of DME pressure, indicating the rapid formation of DME-derived species covering the zeolite surface reacting with the aromatic in the rate-determining step. The kinetics of benzene methylation are consistent with previous studies at higher temperatures with rates extrapolated to zero contact time,[37] and activation energies for toluene methylation are consistent with previous kinetic studies.[52,53] Benzene and toluene methylation proceed with similar rates and activation energies as propene and *n*-butene methylation, respectively, on H-ZSM-5. A comparison of measured rates of aromatic methylation with H-SPP show no significant difference between microporous and mesoporous samples (minimum factor of 150 difference in critical diffusion length) thereby demonstrating that transport restrictions do not play a role in benzene and toluene methylation under the reaction conditions reported in this research.

Methylation of *para*- and *ortho*-xylene show a shift in the predominant surface species from surface methoxides to coadsorbed xylene on surface methoxides, as observed from differing apparent activation energies at low and high partial pressures of xylene. These reactions were run in the absence of isomerization and diffusion limitations, and the formation of surface methoxides for all methylation reactions is consistent with post-reaction titration experiments with water forming 1:1 methanol molecules per zeolite Al. Inhibited DME isotopic exchange is observed for *para*-xylene methylation only, indicative of coadsorbed xylene molecules blocking the methoxide species from further reactions with DME. Observed secondary kinetic isotope effects for benzene, toluene, and xylene methylation studies over H-MFI show that the rate-determining step is the same across these aromatics and involves a transition from sp^3 hybridization to sp^2 hybridization of the surface methoxide in the transition state, which is consistent with that observed for ethylene methylation.[43] These experiments explain the distinct behavior of xylene methylation from benzene and toluene methylation over microporous and mesoporous MFI on a mechanistic basis.

■ ASSOCIATED CONTENT

Supporting Information

Thiele moduli for methylation reactions over H-ZSM-5 and H-SPP, and rate and energetic consequences at low and high xylene partial pressures over H-ZSM-5 and H-SPP. This material is available free of charge via the Internet at http://pubs.acs.org.

■ AUTHOR INFORMATION

Corresponding Author

*E-mail: abhan@umn.edu.

Notes

The authors declare no competing financial interest.

■ ACKNOWLEDGMENTS

The authors acknowledge financial support from The Dow Chemical Company and the National Science Foundation (CBET 1055846)

■ REFERENCES

(1) Chang, C. D. *Catal. Rev. Sci. Eng.* **1983**, *25*, 1−118.
(2) Chang, C. D.; Kuo, J. C. W.; Lang, W. H.; Jacob, S. M.; Wise, J. J.; Silvestri, A. J. *Ind. Eng. Chem. Process Des. Dev.* **1978**, *17*, 255−260.
(3) Chang, C. D.; Silvestri, A. J. *J. Catal.* **1977**, *47*, 249−259.
(4) Song, W. G.; Marcus, D. M.; Fu, H.; Ehresmann, J. O.; Haw, J. F. *J. Am. Chem. Soc.* **2002**, *124*, 3844−3845.
(5) Olsbye, U.; Bjorgen, M.; Svelle, S.; Lillerud, K. P.; Kolboe, S. *Catal. Today* **2005**, *106*, 108−111.
(6) Svelle, S.; Joensen, F.; Nerlov, J.; Olsbye, U.; Lillerud, K.; Kolboe, S.; Bjorgen, M. *J. Am. Chem. Soc.* **2006**, *128*, 14770−14771.
(7) Marcus, D. M.; McLachlan, K. A.; Wildman, M. A.; Ehresmann, J. O.; Kletnieks, P. W.; Haw, J. F. *Angew. Chem., Int. Ed.* **2006**, *45*, 3133−3136.
(8) Lesthaeghe, D.; Van Speybroeck, V.; Marin, G. B.; Waroquier, M. *Ind. Eng. Chem. Res.* **2007**, *46*, 8832−8838.
(9) Lesthaeghe, D.; Van Speybroeck, V.; Marin, G. B.; Waroquier, M. *Angew. Chem., Int. Ed.* **2006**, *45*, 1714−1719.
(10) Lesthaeghe, D.; Van Speybroeck, V.; Marin, G. B.; Waroquier, M. *Chem. Phys. Lett.* **2006**, *417*, 309−315.
(11) Dessau, R. M.; LaPierre, R. B. *J. Catal.* **1982**, *78*, 136−141.
(12) Dessau, R. M. *J. Catal.* **1986**, *99*, 111−116.
(13) Dessau, R. M. *J. Catal.* **1987**, *103*, 526−528.
(14) Dahl, I. M.; Kolboe, S. *J. Catal.* **1996**, *161*, 304−309.
(15) Dahl, I. M.; Kolboe, S. *J. Catal.* **1994**, *149*, 458−464.
(16) Dahl, I. M.; Kolboe, S. *Catal. Lett.* **1993**, *20*, 329−336.
(17) Cui, Z.; Liu, Q.; Ma, Z.; Bian, S.; Song, W. *J. Catal.* **2008**, *258*, 83−86.
(18) Cui, Z.; Liu, Q.; Song, W.; Wan, L. *Angew. Chem., Int. Ed.* **2006**, *45*, 6512−6515.
(19) Svelle, S.; Ronning, P. O.; Olsbye, U.; Kolboe, S. *J. Catal.* **2005**, *234*, 385−400.
(20) Svelle, S.; Ronning, P. A.; Kolboe, S. *J. Catal.* **2004**, *224*, 115−123.
(21) Haw, J. F.; Song, W. G.; Marcus, D. M.; Nicholas, J. B. *Acc. Chem. Res.* **2003**, *36*, 317−326.
(22) Haw, J. F.; Nicholas, J. B.; Song, W. G.; Deng, F.; Wang, Z. K.; Xu, T.; Heneghan, C. S. *J. Am. Chem. Soc.* **2000**, *122*, 4763−4775.
(23) McCann, D. M.; Lesthaeghe, D.; Kletnieks, P. W.; Guenther, D. R.; Hayman, M. J.; Van Speybroeck, V.; Waroquier, M.; Haw, J. F. *Angew. Chem., Int. Ed.* **2008**, *47*, 5179−5182.
(24) Song, W. G.; Haw, J. F.; Nicholas, J. B.; Heneghan, C. S. *J. Am. Chem. Soc.* **2000**, *122*, 10726−10727.
(25) Mikkelsen, O.; Ronning, P. O.; Kolboe, S. *Microporous Mesoporous Mater.* **2000**, *40*, 95−113.
(26) Teketel, S.; Olsbye, U.; Lillerud, K.; Beato, P.; Svelle, S. *Microporous Mesoporous Mater.* **2010**, *136*, 33−41.
(27) Wang, C.; Wang, Y.; Xie, Z.; Liu, Z. *J. Phys. Chem. C* **2009**, *113*, 4584−4591.
(28) Bjorgen, M.; Olsbye, U.; Petersen, D.; Kolboe, S. *J. Catal.* **2004**, *221*, 1−10.
(29) Kolboe, S.; Svelle, S.; Arstad, B. *J. Phys. Chem. A* **2009**, *113*, 917−923.
(30) Lesthaeghe, D.; De Sterck, B.; Van Speybroeck, V.; Marin, G. B.; Waroquier, M. *Angew. Chem., Int. Ed.* **2007**, *46*, 1311−1314.
(31) Ilias, S.; Bhan, A. *ACS Catal.* **2013**, *3*, 18−31.
(32) Ilias, S.; Bhan, A. *J. Catal.* **2012**, *290*, 186−192.
(33) Bjorgen, M.; Olsbye, U.; Svelle, S.; Kolboe, S. *Catal. Lett.* **2004**, *93*, 37−40.
(34) Bjorgen, M.; Olsbye, U.; Kolboe, S. *J. Catal.* **2003**, *215*, 30−44.
(35) Bjorgen, M.; Svelle, S.; Joensen, F.; Nerlov, J.; Kolboe, S.; Bonino, F.; Palumbo, L.; Bordiga, S.; Olsbye, U. *J. Catal.* **2007**, *249*, 195−207.
(36) Arstad, B.; Kolboe, S. *J. Am. Chem. Soc.* **2001**, *123*, 8137−8138.
(37) Van der Mynsbrugge, J.; Visur, M.; Olsbye, U.; Beato, P.; Bjorgen, M.; Van Speybroeck, V.; Svelle, S. *J. Catal.* **2012**, *292*, 201−212.
(38) Ahn, J. H.; Kolvenbach, R.; Al-Khattaf, S. S.; Jentys, A.; Lercher, J. A. *ACS Catal.* **2013**, *3*, 817−825.
(39) Arstad, B.; Kolboe, S.; Swang, O. *J. Phys. Chem. B* **2002**, *106*, 12722−12726.
(40) Svelle, S.; Arstad, B.; Kolboe, S.; Swang, O. *J. Phys. Chem. B* **2003**, *107*, 9281−9289.
(41) Svelle, S.; Kolboe, S.; Swang, O.; Olsbye, U. *J. Phys. Chem. B* **2005**, *109*, 12874−12878.
(42) Vos, A.; Rozanska, X.; Schoonheydt, R.; van Santen, R.; Hutschka, F.; Hafner, J. *J. Am. Chem. Soc.* **2001**, *123*, 2799−2809.
(43) Hill, I. M.; Hashimi, S. A.; Bhan, A. *J. Catal.* **2012**, *285*, 115−123.
(44) Hill, I. M.; Hashimi, S. A.; Bhan, A. *J. Catal.* **2012**, *291*, 155.
(45) Hill, I. M.; Ng, Y. S.; Bhan, A. *ACS Catal.* **2012**, *2*, 1742−1748.
(46) Zhang, X.; Liu, D.; Xu, D.; Asahina, S.; Cychosz, K. A.; Agrawal, K. V.; Al Wahedi, Y.; Bhan, A.; Al Hashimi, S.; Terasaki, O.; Thommes, M.; Tsapatsis, M. *Science* **2012**, *336*, 1684−1687.
(47) Berger, R.; Perez-Ramirez, J.; Kapteijn, F.; Moulijn, J. *Chem. Eng. J.* **2002**, *90*, 173−183.
(48) Van Speybroeck, V.; Van der Mynsbrugge, J.; Vandichel, M.; Hemelsoet, K.; Lesthaeghe, D.; Ghysels, A.; Marin, G. B.; Waroquier, M. *J. Am. Chem. Soc.* **2011**, *133*, 888−899.
(49) Svelle, S.; Tuma, C.; Rozanska, X.; Kerber, T.; Sauer, J. *J. Am. Chem. Soc.* **2009**, *131*, 816−825.
(50) Pope, C. G. *J. Phys. Chem.* **1984**, *88*, 6312−6313.
(51) Pope, C. G. *J. Phys. Chem.* **1986**, *90*, 835−837.
(52) Vinek, H.; Lercher, J. A. *J. Mol. Catal.* **1991**, *64*, 23−39.
(53) Rabiu, S.; Al-Khattaf, S. *Ind. Eng. Chem. Res.* **2008**, *47*, 39−47.
(54) Odedairo, T.; Balasamy, R. J.; Al-Khattaf, S. *Ind. Eng. Chem. Res.* **2011**, *50*, 3169−3183.
(55) Cejka, J.; Zilkova, N.; Wichterlova, B.; Eder-Mirth, G.; Lercher, J. A. *Zeolites* **1996**, *17*, 265−271.
(56) Armaroli, T.; Bevilacqua, M.; Trombetta, M.; Alejandre, A.; Ramirez, J.; Busca, G. *Appl. Catal., A* **2001**, *220*, 181−190.
(57) Ruthven, D. M. *Adsorption* **2007**, *13*, 225−230.
(58) Ruthven, D. M.; Eic, M.; Richard, E. *Zeolites* **1991**, *11*, 647−653.
(59) Ruthven, D. M.; Vidoni, A. *Chem. Eng. Sci.* **2012**, *71*, 1−4.
(60) Jentys, A.; Tanaka, H.; Lercher, J. *J. Phys. Chem. B* **2005**, *109*, 2254−2261.
(61) Gobin, O. C.; Reitmeier, S. J.; Jentys, A.; Lercher, J. A. *Microporous Mesoporous Mater.* **2009**, *125*, 3−10.
(62) Pope, C. G. *J. Chem. Soc., Faraday Trans.* **1993**, *89*, 1139−1141.
(63) Chen, W.; Tsai, T.; Jong, S.; Zhao, Q.; Tsai, C.; Wang, I.; Lee, H.; Liu, S. *J. Mol. Catal. A: Chem.* **2002**, *181*, 41−55.
(64) Xiao, J. R.; Wei, J. *Chem. Eng. Sci.* **1992**, *47*, 1143−1159.
(65) Roquemalherbe, R.; Wendelbo, R.; Mifsud, A.; Corma, A. *J. Phys. Chem.* **1995**, *99*, 14064−14071.
(66) Xiao, J. R.; Wei, J. *Chem. Eng. Sci.* **1992**, *47*, 1123−1141.
(67) Svelle, S.; Visur, M.; Olsbye, U. *Top. Catal.* **2011**, *54*, 897−906.
(68) Lesthaeghe, D.; Van der Mynsbrugge, J.; Vandichel, M.; Waroquier, M.; Van Speybroeck, V. *ChemCatChem* **2011**, *3*, 208−212.
(69) Yamazaki, H.; Shima, H.; Imai, H.; Yokoi, T.; Tatsumi, T.; Kondo, J. N. *Angew. Chem., Int. Ed.* **2011**, *50*, 1853−1856.
(70) Wang, W.; Hunger, M. *Acc. Chem. Res.* **2008**, *41*, 895−904.
(71) Bosacek, V. *J. Phys. Chem.* **1993**, *97*, 10732−10737.
(72) Boronat, M.; Martinez, C.; Corma, A. *Phys. Chem. Chem. Phys.* **2011**, *13*, 2603−2612.
(73) Zicovich-Wilson, C. M.; Viruela, P.; Corma, A. *J. Phys. Chem.* **1995**, *99*, 13224−13231.
(74) Cheung, P.; Bhan, A.; Sunley, G. J.; Law, D. J.; Iglesia, E. *J. Catal.* **2007**, *245*, 110−123.
(75) Brogaard, R. Y.; Weckhuysen, B. M.; Nørskov, J. K. *J. Catal.* **2013**, *300*, 235−241.
(76) Mukti, R. R.; Jentys, A.; Lercher, J. A. *J. Phys. Chem. C* **2007**, *111*, 3973−3980.
(77) Takaishi, T.; Tsutsumi, K.; Chubachi, K.; Matsumoto, A. *J. Chem. Soc., Faraday Trans.* **1998**, *94*, 601−608.

(78) Lee, C.; Chiang, A. *J. Chem. Soc., Faraday Trans.* **1996**, *92*, 3445−3451.
(79) Mentzen, B. F. *Mater. Res. Bull.* **1992**, *27*, 953−960.
(80) Nair, S.; Tsapatsis, M. *J. Phys. Chem. B* **2000**, *104*, 8982−8988.
(81) Li, Y.; Jun, H. *Appl. Catal., A* **1996**, *142*, 123−137.